Published in final edited form as:
Cell Microbiol. 2013 September ; 15(9): 1508–1526. doi:10.1111/cmi.12124.

Plasmodium yoelii inhibitor of cysteine proteases is exported to exomembrane structures and interacts with yoelipain-2 during asexual blood stage development

Ying Pei[#1], **Jessica L. Miller**[#1], **Scott E. Lindner**[1], **Ashley M. Vaughan**[1], **Motomi Torii**[2], and **Stefan H. I. Kappe**[1,3,#]

[1]Seattle Biomedical Research Institute, 307 Westlake Avenue North, Suite 500, Seattle, WA 98109, USA

[2]Department of Molecular Parasitology, Ehime University Graduate School of Medicine, Toon, Ehime 791-0295, Japan

[3]Department of Global Health, University of Washington, Seattle, WA, 98195, USA

[#] These authors contributed equally to this work.

Summary

Plasmodium falciparum (Pf) blood stages express falstatin, an inhibitor of cysteine proteases (ICP), which is implicated in regulating proteolysis during red blood cell infection. Recent data using the *Plasmodium berghei* rodent malaria model suggested an additional role for ICP in the infection of hepatocytes by sporozoites and during liver stage development. Here we further characterize the role of ICP *in vivo* during infection with *Plasmodium yoelii* (Py) and Pf. We found that Py-ICP was refractory to targeted gene deletion indicating an essential function during asexual blood stage replication, but significant down-regulation of ICP using a regulated system did not impact blood stage growth. Py-ICP localized to vesicles within the asexual blood stage parasite cytoplasm, the parasitophorous vacuole, and was exported to dynamic exomembrane structures in the infected erythrocyte. In sporozoites, expression was observed in rhoptries, in addition to intracellular vesicles distinct from TRAP containing micronemes. During liver stage development, Py-ICP was confined to the parasite compartment until the final phase of liver stage development when, after parasitophorous vacuole membrane breakdown, it was released into the infected hepatocyte. Finally, we identified the cysteine protease yoelipain-2 as a binding partner of Py-ICP during blood stage infection. These data show that ICP may be important in regulating proteolytic processes during blood stage development, and is likely playing a role in liver stage-hepatocyte interactions at the time of exoerythrocytic merozoite release.

Introduction

Plasmodium parasites undergo a complex life cycle between their mosquito vector and mammalian host, which entails numerous host invasion, replication, and egress events. Following an infectious mosquito bite, *Plasmodium* sporozoites actively migrate to the blood stream and are transported to the liver, where they invade hepatocytes. In the hepatocyte, the parasites form a vacuolar compartment (the parasitophorous vacuole, PV), within which they grow and develop as liver stages. Liver stages undergo significant replication, leading to an enormous increase in parasite biomass, culminating in the release

[#]To whom correspondence should be addressed. Tel.: +1-206-256-7205; fax: +1-206-256-7229; stefan.kappe@seattlebiomed.org.

Conflict of interest The authors have no conflict of interest to declare.

of 10,000-50,000 infectious exoerythrocytic merozoites. These merozoites egress into the blood stream and invade RBCs, initiating the asexual intraerythrocytic replication cycle of repeated waves of invasion, growth, and egress of new merozoites (Lindner *et al.*, 2012). Parasite proteases play important and essential roles during the life cycle of the parasite and are the targets of anti-malarial therapy development (Shenai *et al.*, 2002, Lee *et al.*, 2003, Na *et al.*, 2004, Rosenthal, 2004, Micale *et al.*, 2006, Singh *et al.*, 2006).

Proteases have been best studied in the asexual erythrocytic infection cycle of the human parasite *P. falciparum*. Much less is known about the roles of parasite proteases during liver stage infection, even though they are expressed during this life cycle stage (Tarun *et al.*, 2008). Some of the best studied *Plasmodium* proteases are the falcipains. To date, four of these cysteine proteases have been identified and characterized: falcipain-1, falcipains-2A and -2B, and falcipain-3 (Salas *et al.*, 1995, Francis *et al.*, 1996, Shenai *et al.*, 2000, Sijwali *et al.*, 2001). Gene deletion and inhibitor studies showed that falcipain-2 and falcipain-3 play essential roles in hemoglobin hydrolysis and merozoite egress in blood stages (Sijwali *et al.*, 2001, Sijwali *et al.*, 2004b, Dasaradhi *et al.*, 2005, Hogg *et al.*, 2006, Subramanian *et al.*, 2009). While falcipain-1 is not essential for hemoglobin degradation, it is important for oocyst maturation in the mosquito (Eksi *et al.*, 2004, Sijwali *et al.*, 2004a, Kumar *et al.*, 2007). Due to their essentiality in different life cycle stages, falcipain inhibitors are potential anti-malarial drug candidates (Lee *et al.*, 2003, Desai *et al.*, 2004, Desai *et al.*, 2006, Micale *et al.*, 2006). Other cysteine proteases has been implicated in the egress of sporozoites from the oocyst during parasite mosquito stage development (Aly *et al.*, 2005). In addition, a papain family cysteine protease cleaves the major surface sporozoite protein, circumsporozoite protein (CSP), which is essential for sporozoite invasion (Coppi *et al.*, 2005). In liver stages, the papain-like cysteine protease, serine repeat antigen 3 (SERA3), was shown to be released into host hepatocyte during late liver stage development and was suggested to contribute to parasitophorous vacuole membrane (PVM) disruption and merozoite release (Schmidt-Christensen *et al.*, 2008). Despite the important roles of proteases in all stages of the parasite life cycle, it remains unclear how *Plasmodium* regulates its own protease activities, or potentially those of host cell proteases.

An endogenous Pf cysteine protease inhibitor, Pf-ICP (PF3D7_0911900; Falstatin), was previously identified via a BLAST search of the Pf genome using the *Trypanosoma cruzi* cysteine protease inhibitor chagasin as a query (Pandey *et al.*, 2006). A recombinant Pf-ICP expressed in *E. coli* was shown to potently inhibit a number of host proteases by *in vitro* protease activity assays. Additionally, Pf-ICP also inhibited several parasite proteases in these assays, including falcipain-2 and falcipain-3, but not falcipain-1. However, the *in vivo* relevance of these interactions remains unclear. Furthermore, a polyclonal Pf-ICP antibody inhibited merozoite RBC invasion (Pandey *et al.*, 2006). Recently, *P. berghei* (Pb) ICP was characterized (Rennenberg *et al.*, 2010). Pb-ICP localized to sporozoite micronemes and was secreted in trails during gliding motility. The study further suggested that Pb-ICP plays a role in hepatocyte invasion and is important in suppressing host cell apoptosis during liver stage development (Rennenberg *et al.*, 2010).

Here we identify an ortholog of ICP in Py (Py-ICP), and analyzed this protease inhibitor throughout the parasite life cycle. We show that Py-ICP is expressed during the intra-erythrocytic stages of development where it localized to the PV as well as to parasite exomembrane structures that extend into the infected RBC cytoplasm. We also show that Py-ICP interacts with the protease yoelipain-2, the ortholog of falcipain-2 *in vivo*. In pre-erythrocytic stages, Py-ICP differed from Pb-ICP in that it was localized in sporozoite rhoptries and was not deposited in trails during gliding motility. We find no evidence that ICP is exported beyond the PVM during liver stage development, but observed its release into the infected hepatocyte after PVM breakdown.

Results

Identification of the ICP ortholog in Py

ICP is conserved among numerous *Plasmodium* species. However, a Py-ICP ortholog had not been annotated in PlasmoDB (www.plasmodb.org). To determine if Py contained an ICP ortholog, we conducted a BLAST search of the Py genome using Pf-ICP as the query and observed highly conserved nucleotide sequences at the C-terminal region of a 7.3 kb gene, PY03424. We determined that PY03424 was composed of two separate genes (Figure 1 A): a single exon gene we now term PY03424* and Py-ICP. The re-annotated Py-ICP gene has 85% and 34% amino acid identity to its orthologs in Pb and Pf, respectively (Figure 1B). Furthermore, a 1kb Py-ICP transcript was amplified from blood stage parasites by reverse transcriptase (RT)-PCR using primers specific for the Py-ICP 5′ and 3′ un-translated regions (Figure 1C). This 1kb RT-PCR product was the expected size for the spliced Py-ICP transcript consisting of the 1.5kb open reading frame minus the 0.5kb intron (Figure 1A, C).

To track the expression and localization of Py-ICP throughout the parasite life cycle, we generated a transgenic Py line expressing myc epitope-tagged ICP under the control of its endogenous 5′ promoter (Figure S1A). A quadruple c-myc tag was fused to the C-terminus of a second copy of Py-ICP and was integrated into the parasite's genome using a previously reported single crossover insertion strategy (Vaughan *et al.*, 2009). We also generated polyclonal rabbit antisera against purified recombinant Py-ICP expressed in *E. coli*. The specificity of the antisera was first tested by immunofluorescence assay (IFA) on Py-ICP-myc parasites and showed an indistinguishable staining pattern when compared with the anti-myc antibody (Figure S1B), indicating highly specific reactivity. Anti-myc staining also co-localized with previously generated antisera against Pf-ICP (Pandey *et al.*, 2006) (Figure S1C). The specificity of the Py-ICP antisera (Py-ICP AB) was also tested via western blotting on WT and Py-ICP-myc parasite lysate, showing two specific bands in WT parasite lysate (55 kDa and 32 kDa). As Py-ICP-myc parasites contain both native and myc-tagged copies of Py-ICP, western blotting with the Py-ICP antibody identified both the untagged protein as well the higher molecular weight myc-tagged protein (Figure S1D). The Py-ICP antisera also specifically recognized recombinant Py-ICP antigen in western blots (data not shown).

Py-ICP localization in infected erythrocytes

We determined the localization of Py-ICP-myc by IFA during asexual blood stage development using a monoclonal anti-myc antibody and co-staining with an antibody against merozoite surface protein 1 (MSP1). In maturing schizonts, Py-ICP was diffusely distributed within the parasite but showed punctate areas of stronger stained foci (Figure 2A). This is similar to the previously reported expression pattern of Pf-ICP in schizont stages (Pandey *et al.*, 2006). In addition, we tested the localization of ICP in relation to the rhoptry neck protein RON4 (Alexander *et al.*, 2006) (Figure 2 B) and found that the foci of strong ICP staining closely abutted RON4 staining but the staining did not significantly overlap. Free, invading merozoites strongly expressed ICP as well, with the majority of signal focused in the part of the merozoites that faced the target erythrocyte (Figure 2C). To further study the subcellular localization of Py-ICP during intra-erythrocytic development, we used Py-ICP antisera to localize ICP in IFAs and immunoelectron microscopy (IEM). During ring/trophozoite stage, Py-ICP was contained within the parasite but was also partially co-localized with the PVM marker Hep17 (Figure 2D, E, F). Notably, extensions of the PV that projected into the infected erythrocyte were strongly stained for ICP and Hep17. Interestingly, Py-ICP was also observed in structures that were Hep17 negative (Figure 2E, yellow arrow) or inside Hep17 positive distal structures, which appeared connected to the PV (Figure 2D, E, F). To further elucidate the nature of these structures, we conducted IEM

of intra-erythrocytic parasites (Figure 2G). This showed Py-ICP associated with vesicles within the parasite cytoplasm (Figure 2G i) and also localized Py-ICP to the PV (Figure 2G ii). Py-ICP was frequently associated with polymorphic exomembrane structures that appeared segregated in the infected erythrocyte cytoplasm (Figure 2G iii), but might be continuous with the PVM.

In order to observe Py-ICP localization in live parasite-infected cells, we generated a recombinant parasite line expressing Py-ICP fused to a Regulated Fluorescent Affinity (RFA) tag containing a GFP cassette and HA epitope tag (Py-ICP-RFA) (Supplementary Figure S1D and S2) (Muralidharan *et al.*, 2011). Erythrocytes infected with Py-ICP-RFA were immobilized on poly-lysine slides coated with an antibody against the red blood cell marker Ter-119. Py-ICP-RFA localized throughout the parasite and was concentrated in exomembrane structures, confirming the findings on fixed cells. Interestingly, these structures were highly dynamic in nature and were observed moving within the infected erythrocyte (Figure 2H and Supplementary Movies 1 and 2).

Py-ICP is proteolytically processed

Endogenous Py-ICP consistently resolved as two bands in western blots with blood stage parasites when probed with Py-ICP antisera antibodies (Figure 3A and S1D). Cleavage of Py-ICP-myc and Py-ICP-RFA in transgenic blood stages was also observed via western blotting (Figure S1D and S2D). Furthermore, recombinant *E. coli*-expressed Py-ICP also identified as two protein species by Coomassie staining on SDS-PAGE gels (Figure 3B), showing that Py-ICP is similarly processed during expression in *E. coli*. Mass spectrometry analysis identified the higher molecular mass band (~55 kDa) as full-length Py-ICP and the lower molecular mass band (~30 kDa) as the C-terminal portion of Py-ICP (Figure S3A and B). N-terminal sequencing showed that *E. coli*-expressed Py-ICP is cleaved upstream of the methionine at position 178 (Figure 3C). It is unlikely that the two protein species are the product of alternatively spliced Py-ICP transcripts as only a single transcript species was amplified from blood stage parasites Py-ICP mRNA by RT-PCR (Figure 1C).

Pf-ICP is processed and has a similar expression to Py-ICP in blood stages

The Py-ICP antibody was also used to study Pf-ICP expression in blood stages (Figure 4). Western blots of Pf lysate revealed the Pf-ICP resolved into both high and low molecular weight bands, indicating that, Pf-ICP is also processed (Figure 4A). Furthermore, in asexual blood stage parasites, Pf-ICP was observed associated with the PV and in exomembrane structures beyond the confines of the PV (Figure 4B and 4C), similar to the distribution in Py blood stage parasites (Figure 2). Interestingly, most of the Pf-ICP positive structures were not positive for the PV marker exported protein 2 (EXP2), (Figure 4B), suggesting that in Pf, ICP localizes more frequently to exomembranes that are disconnected from the PV.

Py-ICP is expressed in sporozoite rhoptries and is not secreted prior to host cell invasion

We next studied the expression of Py-ICP in mosquito stage parasites. Py-ICP-myc expression was observed by IFA in parasite oocysts, oocyst sporozoites, and salivary gland sporozoites (Figure S4 and Figure 5). Utilizing circumsporozoite protein (CSP) as a marker of the sporozoite surface, distribution of Py-ICP was observed in the interior of both oocyst and salivary gland sporozoites, predominantly on one end of the parasite and excluding the nuclear region (Figure S4 and Figure 5A). Py-ICP partially co-localized with the micronemal protein thrombospondin-related anonymous protein (TRAP) in the sporozoite. However, unlike TRAP, ICP was not secreted from sporozoites when microneme release was triggered (Figure 5B). IEM of salivary gland sporozoites localized Py-ICP to the rhoptries, as well as dispersed in the sporozoite interior, and associated with densely packed

vesicles (Figure 5C). Py-ICP was processed in sporozoites as determined by western blot on Py sporozoite lysate using the Py-ICP AB (Figure 5D).

Previous studies observed that Pb-ICP is secreted in gliding trails during sporozoite motility (Rennenberg *et al.*, 2010). Sporozoite proteins, such as CSP and TRAP, which are present in trails, are necessary for motility and are proteolytically processed by cysteine proteases (Coppi *et al.*, 2005). To investigate whether Py-ICP is secreted in trails during gliding motility, Py sporozoites were allowed to move on glass slides. A monoclonal CSP antibody was used to label the sporozoite surface and trails of shed CSP left behind during motility. In contrast, Py-ICP was observed only inside sporozoites and was not observed in trails during motility (Figure 5E). To verify the absence of Py-ICP in trails, Py-ICP-myc salivary gland sporozoites were used in the same assay and anti-myc antibodies were used to show Py-ICP-myc localization. No Py-ICP-myc was detected in trails further substantiating that Py-ICP is unlikely to be deposited during sporozoite locomotion (Figure 5F). Additionally, we tested for the presence of Pb- (Figure 5G) and Pf-ICP (data not shown) in sporozoite gliding trails by imaging with the Py-ICP antibody. Again, ICP was detected within sporozoites but not in trails. To determine if Py-ICP is exposed externally and could be targeted by antibodies during host cell invasion, we analyzed sporozoite infection of hepatoma cells in the presence of the Py-ICP antisera (Figure 5H). Invaded cells were identified via flow cytometry using a fluorescently labeled antibody against Py-CSP (Kaushansky *et al.*, 2012). Approximately 2% of HepG2-CD81 cells were invaded in the absence of antisera, or in the presence of pre-immune sera (0.1mg/ml). Addition of Py-ICP antisera (0.1mg/ml) did not reduce this invasion rate. In contrast, the same concentration of anti-CSP antibodies reduced sporozoite invasion to approximately 0.5% (Figure 5H).

Py-ICP enters the infected hepatocyte cytoplasm during late liver stage development

In order to examine the expression of Py-ICP during liver stage development, HepG2-CD81 cells were infected with Py-ICP-myc salivary gland sporozoites and liver stages were analyzed by IFA at 4-, 24-, and 43-hr post infection (pi). Parasites were co-stained with antibodies against the PVM marker UIS4 and the parasite cytoplasmic marker HSP70 (Figure S5). During early (4 hr pi) and mid stage (24 hr pi) *in vitro* liver stage infection, Py-ICP-myc localized within the parasite, but was not observed outside the confines of the parasite compartment or in UIS4 positive projections of the PV (Figure S5A and S5B). However, during late liver stage development (43 hr pi), Py-ICP was strongly detected in the host hepatocyte cytoplasm (Figure S5C). To confirm our observations on the dynamics of Py-ICP expression during *in vitro* liver stage development, we next studied Py-ICP liver stage expression and localization *in vivo*. BALB/c mice were injected intravenously with Py-ICP-myc salivary gland sporozoites. Livers of these infected mice were isolated at multiple time-points pi (2-, 16-, 24-, 30-, 43- and 52 hr), fixed, sectioned, and analyzed by IFA to visualize localization of Py-ICP throughout liver stage development (Figure 6). At 2 hr pi, when liver stage parasites are still sporozoite-shaped, Py-ICP was detected inside the parasite only but not in the UIS4-positive PV (Figure 6A). Similarly, during mid-liver stage development (16 hr and 24 hr pi), Py-ICP was distributed ubiquitously within the parasite. Py-ICP was also increasingly associated with the PV as indicated by co-localization with the PVM protein UIS4. This suggests that ICP is released into the PV but is not exported beyond the PVM (Figure 6B and 6C). At 30 hr pi, Py-ICP appeared to be concentrated in vesicular structures that localized to the periphery of all liver stage parasites, close to the PV (Figure 6D). A similar distribution was observed in 40% of infected cells during late liver stages (43 hr pi) (Figure 6E). However, in the majority of late liver stages at 43 hr pi (60%), Py-ICP accumulated in the cytoplasm of the infected hepatocyte, and this was associated with the partial breakdown of the PVM as indicated by discontinuous Hep17 staining (Figure 6F). This localization persisted during further liver stage development up to the

formation of exoerythrocytic merozoites, which at 52 hr pi completely occupied the infected hepatocyte cytoplasm (Figure 6G). Individual exoerythrocytic merozoites that were found in the surrounding liver tissue carried Py-ICP on their surface (Figure 6H), as shown by the co-localization of MSP1 with Py-ICP.

ICP has similar expression profiles in Pf and Py liver stages

To study Pf-ICP during liver stage development, we infected FRG huHep mice, in which livers were repopulated with human hepatocytes (Azuma *et al.*, 2007) with Pf sporozoites. We have previously established that this model supports complete *Pf* liver stage development and can produce a subsequent blood stage infection *ex vivo* (Vaughan *et al.*, 2012). Infected livers were harvested 3 and 7 days pi and liver sections were imaged with Py-ICP antisera and antibodies against Pf-CSP and Pf-MSP1, respectively (Figure 7A, B). Pf-ICP was detected within the liver stages and in a predominantly circumferential pattern in the 3 day liver stage parasite, which is indicative of PV localization (Figure 7A). During late liver stage development, when exoerythrocytic merozoites were observed filling the infected hepatocyte (7 days pi), Pf-ICP was strongly expressed and localized throughout the infected hepatocyte (Figure 7B).

Py-ICP is essential in blood stages

In order to study the importance of ICP during the parasite life cycle we sought to delete the ICP gene in Py asexual blood stage parasites using a double crossover recombination strategy (Figure S6A) (Menard *et al.*, 1997, Vaughan *et al.*, 2009). However, we were unable to obtain double crossover, gene deletion parasites after several independent attempts to transfect parasites with the gene deletion construct (Figure S6A). As an alternative, we attempted to disrupt the Py-ICP open reading frame using a single crossover recombination strategy (Figure S6B). However, this was also unsuccessful and no recombinant parasites were obtained. In a third strategy to manipulate Py-ICP, we generated recombinant parasites expressing a regulated form of ICP (Py-ICP-RFA) (Figure S2). In addition to a GFP cassette, the RFA tag contained an HA epitope and an *E. coli* DHFR degradation domain, which destabilizes the protein in the absence of folate analogs, including trimethoprim (TMP) (Muralidharan *et al.*, 2011). To determine if Py-ICP-RFA could be destabilized *in vivo*, we monitored the average fluorescence intensity of GFP from RFA tagged parasites over time. TMP was administered in the drinking water of mice 24 hrs prior to inoculation with Py-ICP-RFA infected erythrocytes. Two days post infection drug was removed from a subset of mice, while the remaining mice were maintained on TMP for four additional days. The average fluorescence intensity of GFP from 5×10^7 Py-ICP-RFA infected erythrocytes was determined at varying time points using a fluorescence microplate reader. After removal of TMP, GFP fluorescence intensity from Py-ICP-RFA parasites decreased over time, reaching a maximum reduction of 30% as compared to TMP stabilized protein by 72 and 96 hr (Figure 8 A). Protein degradation was also monitored by western blot, which revealed up to a 50% decrease in total ICP protein levels during blood stage replication *in vivo* (Figure 8B and C). Both the full length and processed form of Py-ICP were reduced following removal of TMP. However, this down-regulation was more pronounced in the processed form, which exhibited more than a 5-fold decrease as compared to a 1.7-fold reduction of full length Py-ICP (Figure 8C). However, this reduction was not sufficient to decrease the viability of the recombinant parasite, as there was no detectable difference in blood stage growth *in vivo* in the absence of TMP (Figure 8D). Thus, a larger decrease in protein expression is likely necessary to impact parasite replication and reveal a phenotype of ICP depletion in blood stage parasites. Successful integration of constructs that created Py-ICP-myc and Py-ICP-RFA into the ICP locus by either single crossover (Figure S1A) or double crossover recombination (Figure S2A) demonstrated that that the locus is accessible to

construct integration. Therefore, the inability to delete or disrupt Py-ICP using several independent strategies indicates that Py-ICP has an essential function in blood stages.

Py-ICP interacts with yoelipain-2 in blood stages

Pf- and Pb-ICP were previously shown to bind to and inhibit cysteine protease activity in *in vitro* assays using recombinant proteins (Pandey *et al.*, 2006, Rennenberg *et al.*, 2010). However, ICP *in vivo* interactions with proteases have yet to be determined. To identify binding partners of Py-ICP in blood stages we immunoprecipitated Py-ICP-myc and Py-ICP-RFA from infected erythrocyte protein lysates. Py-ICP-myc was precipitated using an anti-myc antibody, and Py-ICP-RFA was precipitated using an anti-GFP antibody. Interacting proteins were then identified using tandem mass spectrometry. Five independent co-immunoprecipitations, along with four controls (Table S1) were analyzed. The presence of Py-ICP in the immunoprecipitate was confirmed by western blot (Figure S7). Protein hits were considered significant when multiple unique peptides were identified and peptides were present in at least two of the five co-immunoprecipitations, but were absent from all of the control samples (Table 1). Epitope tagged Py-ICP consistently co-immunoprecipitated with the cysteine protease yoelipain-2 (PY00783, the ortholog of falcipain-2 and berghepain-2), and was identified by multiple peptide hits in all 5 co-immunoprecipitations. Other co-immunoprecipitated proteins included two ER-associated proteins, PY03267, the putative ortholog for Rab18 (PY01075), and two scaffolding proteins, PY05916 and PY01361 (Table 1).

Discussion

Our study characterized Py- and Pf-ICP, cysteine protease inhibitors, throughout the parasite life cycle. We show that both Pf- and Py-ICP are exported from the parasite compartment into exomembrane structures during intra-erythrocytic development but are released into the infected hepatocyte only after PVM breakdown in late liver stage infection. Consequently, the modes of interaction of this parasite ICP with host cell components should be distinct in erythrocytic infection and hepatocytic infection, implying that ICP is likely involved in the modulation of unique aspects of the respective host cell environments.

In addition to Py and Pf, Pb also expresses an ICP (Rennenberg *et al.*, 2010), however we observed several features of Py-ICP that differ from previously reported features of Pb-ICP in sporozoites. Pb-ICP was observed in sporozoite trails left behind during gliding motility, and it was shown that it co-localizes with TRAP in micronemes of sporozoites (Rennenberg *et al.*, 2010). In contrast, we show that Py-ICP does not co-localize with TRAP, is not released upon induction of microneme secretion, and is clearly not deposited in trails by gliding sporozoites. Furthermore, we also were unable to identify Pb-ICP in Pb sporozoite gliding trails using the Py-ICP antibody; a surprising finding given previously published results (Rennenberg *et al.*, 2010). Additionally, we detected Py-ICP in the sporozoite rhoptries by IEM, a localization that had not been described for Pb-ICP. Py-ICP was also scattered in the sporozoite interior, and was possibly associated with vesicles. These vesicles could be dense granules, or involved in the transport of ICP to the rhoptries.

Pb-ICP and Py-ICP also differ in their localization during liver stage development. Py-ICP was clearly confined to the liver stage parasite and the PV during early to mid schizont liver stage development both in hepatoma cell infections and in *in vivo* infections in mice. However, Rennenberg *et al.* found that Pb-ICP is exported beyond the liver stage PV into the host hepatocyte, supporting its proposed role in the inhibition of host cell apoptosis (Rennenberg *et al.*, 2010). However exported Pb-ICP was present in an EXP1 positive membrane compartment (Rennenberg *et al.*, 2010), making it difficult to envision a role in interfering with host cell apoptosis at this stage. Thus, we suggest that, like Py-ICP, Pb-ICP

is not secreted into the host cell cytoplasm during liver stage development, but rather is confined within the parasite and the PV. Importantly, our work with Pf shows that Pf-ICP is also confined to the PV during liver stage development. Therefore, if indeed Pb-ICP is exported into the host cell cytoplasm, its expression pattern is not conserved in human malaria parasites.

While there are several discrepancies between the localization of ICP in Py and Pb, it is clearly present in the cytoplasm of the host hepatocyte following PVM breakdown that occurs during late liver stage development in both parasite species. The release of ICP into the host hepatocyte would allow ICP to inhibit host cell proteases and thus would preempt proteolytic attack once the parasite comes into direct contact with the host cell cytoplasm. Previous work on Pf has shown that recombinant Pf-ICP inhibited both host derived cathepsins and caspases *in vitro* (Pandey *et al.*, 2006), both of which are cysteine proteases involved in apoptosis (Turk *et al.*, 2007). However, ICP's ability to inhibit caspases is controversial as a further study did not observe significant inhibitory activity against caspase-3 or caspase-8 (Hansen *et al.*, 2011). During late stage development, the parasite induces a specialized form of cell death in the host hepatocyte that is dependent on cysteine proteases and independent of caspases (Sturm *et al.*, 2006). The mechanism by which the parasite achieves this is unknown, but one possibility is that it utilizes protease inhibitors to inhibit host cathepsins and caspases late in infection and induces apoptosis via its own cysteine proteases. Two studies have suggested that *Plasmodium* can inhibit host cell apoptosis during the early stages of liver infection (Leiriao *et al.*, 2005, van de Sand *et al.*, 2005), but this process likely does not involve Py-ICP due to its parasite compartment-restricted localization at early to mid-time points of liver stage development.

Another potential role of ICP during late liver stage development is in exoerythrocytic merozoite egress from hepatocytes, which, like egress from erythrocytes, might be mediated by regulated protease cascades (Blackman, 2008). ICP could be involved in the spatial and temporal coordination of the proteases necessary for this release. In addition to its localization in the host hepatocyte cytoplasm after PVM rupture, Py-ICP also co-localized with MSP-1 in late liver stage schizonts and was detected on the surface of exoerythrocytic merozoites. This distribution might protect the exoerythrocytic merozoites from attack by host proteases.

Several *Plasmodium* proteases have been implicated in either the breakdown of the PVM, or the host cell structures during merozoite egress from red blood cells (Reviewed in (Blackman, 2008)). One such protease, falcipain-2, digests host cell ankyrin and protein 4.1, components of the RBC cytoskeleton, during intraerythrocytic replication (Dua *et al.*, 2001, Hanspal *et al.*, 2002). Moreover, inhibition of falcipain-2 also inhibited blood stage parasite maturation and merozoite egress (Dhawan *et al.*, 2003), supporting a role for falcipain-2 in parasite egress. Here we identified the *Py* ortholog of falcipain-2, yoelipain-2, as a binding partner of Py-ICP by immunoprecipitation in blood stages. This is the first time that ICP has been shown to interact with a parasite cysteine protease *in vivo*. Interestingly, falcipain-2 is expressed within the parasite as well as in exomembrane structures that extend into the infected erythrocyte cytoplasm (Dhawan *et al.*, 2003), reminiscent of the Py-ICP localization shown herein.

The presence of Py-ICP in exomembrane structures is consistent with the finding that it co-immunoprecipitated with parasite ER associated factors such as Py-Rab18 and an uncharacterized ER biogenesis factor (PY03267). Exomembrane structures are likely derived from the parasite ER and it is likely that ER-associated proteins are maintained during membrane transfer from parasite to host cell. Frequently the exomembrane structures co-localized with the PVM marker Hep17, suggesting that they might be part of the

tubovesicular network, which extends from the PV into the erythrocyte cytoplasm. However, ICP was also found in Hep17 negative structures. Exomembrane structures have been implicated in protein export by blood stage parasites (Wickert *et al.*, 2003). It is tempting to suggest that ICP plays a role in regulating the establishment of the parasite derived intra-erythrocytic membrane network and remodeling of the infected erythrocyte. Importantly, ICP appears to be essential for blood stage parasite survival. Despite several attempts to delete the gene encoding ICP in Py, we consistently failed to isolate a gene knockout, whilst genetic alterations that restored ICP function such as the addition of epitope and fluorescent protein tags where readily obtained. Interestingly, by fusing ICP to a regulated fluorescent affinity (RFA)-tag we achieved ~50% reduction of ICP levels in blood stage parasites, yet no growth phenotype was observed at this level of reduction. The result implies that ICP levels must be more significantly reduced in order to show an impact on blood stage growth. However, accomplishing a greater down regulation of ICP was not possible with currently available tools. Of note, we were not able to recover Py-ICP-RFA sporozoites from infected mosquitoes, suggesting that Py-ICP could be necessary during mosquito stage development. However additional experiments are required to further substantiate this observation.

Together, we have shown here that ICP is important for blood stage parasite growth. This might in part be mediated by its function in regulating protease activities in the parasite-derived intra-erythrocytic membrane network, particularly the activity of falcipain-2 and its rodent orthologs. In pre-erythrocytic stages, ICP localizes to the rhoptries of sporozoites in addition to small vesicles, is not released under conditions that led to secretion of TRAP, and is not deposited in trails during sporozoite locomotion. During most of liver stage development, ICP remains within the confines of the PV, ruling out a role in regulating host hepatocyte apoptosis. Only after PV breakdown is ICP released into the host hepatocyte cytoplasm allowing it to potentially inhibit host proteases. Continued research on ICP and its role in *Plasmodium* development will help to further our understanding of protease and protease inhibitor functions during malaria parasite infection.

Experimental Procedures

Parasite growth and sporozoite isolation

Female six-to-eight week old Swiss Webster (SW) mice were injected with blood stage *17XNL* wild type (WT) parasites to begin the growth cycle. The infected mice were used to feed female *Anopheles stephensi* mosquitoes after gametocyte exflagellation was observed. Ten days after the blood meal, 15-20 mosquitoes were dissected to evaluate midgut oocyst formation. At day 14 or 15 post-blood meal, salivary gland sporozoites were isolated and harvested as previously described (Tarun *et al.*, 2007).

Generation of transgenic parasites expressing Py-ICP-myc

As previously reported (Vaughan *et al.*, 2009), we have generated a b3D-myc vector for epitope tagging genes of interest. To generate the Py-ICP-myc parasite line, approximately 1.5 kb of upstream of the start codon and the entire coding sequence of the Py-ICP gene (except for its stop codon) was amplified by PCR from 17XNL genomic DNA. This PCR product was cloned upstream in-frame with the quadruple myc tag in b3D-myc. The plasmid was subsequently linearized with BsmI and integrated into the Py 17XNL genome using standard procedures (Labaied *et al.*, 2007). This integration strategy created two functional copies of the *Py-ICP* gene, which were both under the control of the endogenous promoter. Genotyping of the Py-ICP-myc parasite by PCR is shown in Figure S1A.

Generation of Py transgenic parasites expressing Py-ICP-RFA

The regulatable, fluorescent affinity (RFA) tag (Muralidharan *et al.*, 2011) consists of GFPmut2, an *E. coli* DHFR degradation domain (DDD) and a single HA epitope. A plasmid bearing the RFA tag [kindly provided by Dr. Daniel Goldberg (Washington University School of Medicine, St. Louis, MO)] served as a template for PCR amplification using primers designed with exogenous restriction sites to facilitate its insertion into the pDEF-HsDHFR plasmid (available from the NIAID/ATCC at www.MR4.org, Cat# MRA-774). The product of this ligation is pDEF+RFA. Sequence coding for the C-terminal 207 amino acids (without stop codon) 621 base pairs of the 3′UTR of *Py-ICP* were PCR amplified from genomic DNA with primers that included exogenous SpeI and NotI restriction sites. These PCR products were combined by splicing by overhang extension SOE PCR, which also introduced an ApaI site between the two products for downstream plasmid linearization prior to transfection (Mikolajczak *et al.*, 2008). This SOE PCR product was digested with NotI and SpeI, and inserted into pDEF+RFA. The resulting plasmid was linearized by digestion with ApaI and transfected by standard methods (Jongco *et al.*, 2006) to yield a double-crossover replacement of the native *Py-ICP* locus that enabled expression of a C-terminal RFA tag. Py-ICP-RFA was propagated in SW mice whose water contained 250μg/ml of TMP (Sigma).

Generation of a polyclonal Py-ICP antibody

The open reading frame of *Py-ICP* minus the signal peptide sequence was amplified from Py 17XNL genomic DNA by the Advantage 2 PCR Kit (Clontech, Mountain View, CA) with the primer set 5′-CCATGGGGTACTCTTTTGACATTGTAAACG-3′ and 5′-CTCGAGTTGGACAGTTACGTATAAAATTTTAGTG-3′. The amplified DNA fragment was digested with *NcoI* and *XhoI* and ligated into the pET28b (+) (Novagen, Gibbstown, NJ) expression vector in frame with the C-terminal 6xHis tag. Recombinant His-tagged Py-ICP was expressed in *E. coli* and subsequently purified using a nickel affinity column and size exclusion chromatography. The purified recombinant protein was sent to Pocono Rabbit Farm and Laboratory Incorporated (Canadensis, PA) for the generation of polyclonal antibodies, which were subsequently affinity purified on a column containing the recombinant antigen and validated by western blotting against the recombinant antigen (data not shown).

Immunoelectron microscopy

Py 17XNL infected mouse blood or infected mosquito salivary glands were fixed in PBS +1% paraformaldehyde/0.2% glutaraldehyde in Hepes-buffered saline, and embedded in LR white resin (Polysciences, Inc., Warrington, PA). Sections were blocked for 30 min in PBS-milk-Tween 20, incubated overnight at 4°C in PBS-milk-Tween 20 containing rabbit anti-Py-ICP serum (1/50 dilution), and then incubated for 1 hour in PBS-milk-Tween 20 containing goat anti-rabbit IgG conjugated with gold particles (15 nm diameter; British BioCell International, Ltd). Sections were examined with a JEM-1230 electron microscope (JEOL, Japan) after staining with 2% uranyl acetate and lead citrate.

Immunofluorescence assays (IFAs)

Blood stages—Blood was harvested from infected SW mice when the percent parasitemia was between 2% and 5%. Blood was diluted one to ten with RPMI-1640 media (HyClone, Logan, UT). Approximately 500 μl of diluted blood was used in each IFA. RBCs were washed twice in 1x PBS and were fixed in 1xPBS containing 4% paraformaldehyde and 0.0075% glutaraldehyde for 30 min at RT, permeabilized with 0.1 % v/v Triton X-100 in 1xPBS for 10 min at RT, and blocked with 3% w/v bovine serum albumin (BSA) in 1xPBS overnight at 4°C. IFAs were performed using primary antibodies including rabbit polyclonal

antibodies against Py merozoite surface protein 1(MSP1 (Farley *et al.*, 1995), 1/100 dilution), Py-ICP (1/1000 dilution), and GFP (1/1000 dilution)(Invitrogen, Carlsbad, CA) and mouse monoclonal antibodies against Py Hep17 (1/100 dilution), HA epitope tag (1/500 dilution) (Roche Applied Science, Indianapolis IN) and the c-myc epitope tag (1/400 dilution) (Santa Cruz Biotechnology, Santa Cruz CA). Incubations with primary antibodies were for 1 hr at RT. Fluorescent staining was achieved with Alexa Fluor-conjugated secondary antibodies (Invitrogen, Carlsbad, CA) specific to rabbit and mouse IgG (1/500 dilution) applied for 30 minutes at RT. Nucleic acid was stained with 2 μg/ml 4′, 6′-diamidino-2-phenylindole (DAPI) for 5 min and the cells were then washed twice in PBS as above. The cells were then dried on a poly-lysine treated slide and were mounted with FluoroGuard anti-fade reagent (Bio-Rad, Hercules, CA). Images were acquired using Olympus 1 × 70 Delta Vision and were deconvolved using Softworx software (Applied Precision).

Salivary gland sporozoites—Salivary gland sporozoites were isolated and fixed with formalin (Sigma, St. Louis, MO) for 10 min at RT. In some cases micronemal secretion was inducted by incubating sporozoites for 30 min in RPMI supplemented with 20% FCS prior to fixation. Fixed sporozoites were applied to a poly-lysine treated slide, which was housed in a wet chamber at 4°C overnight. Sporozoites were washed twice with 1xPBS, permeabilized and blocked with 2 % w/v BSA in 1xPBS plus 0.2 % v/v Triton X-100 in PBS for 1 hr at 37°C. An IFA was performed using a rabbit polyclonal antibody (anti-myc or Py-ICP AB) and a mouse antibody [anti-myc (1/400 dilution), anti-TRAP (1/250 dilution), or anti-CSP (1/100 dilution)]. Fluorescent staining, microscopy, and deconvolution were conducted as described above.

Liver stages—To visualize *in vivo* development of Py-ICP-myc parasites in livers, six-to-eight week old female BALB/c mice (Harlan laboratories) were injected intravenously with 10^6 Py-ICP-myc sporozoites. Livers were removed from infected mice at time points post infection (pi) (2-, 16-, 24-, 30-, 43- and 52-hr), washed extensively with 1xPBS, and fixed in 4 % v/v paraformaldehyde in 1xPBS. Fifty-micrometer sections were cut from fixed livers using a Vibratome apparatus (Ted Pella Inc., Redding, CA). IFAs were performed as previously described (Vaughan *et al.*, 2009). Primary antibodies used in IFAs were rabbit polyclonal antibodies against the c-myc epitope (1/100 dilution), Py UIS4 (1/40 dilution), Py MSP1 (1/100 dilution) and Py-ICP paired with mouse monoclonal antibodies against Py CSP (1/100 dilution), the c-myc epitope (1/100 dilution) and Py Hep17 (1/50 dilution). To study the expression of ICP in human parasites, FRG huHep mice with humanized livers (Azuma *et al.*, 2007) were injected with 10^6 WT Pf sporozoites and the infected livers were harvested at 3 and 7 days pi. IFA was performed following similar procedures as described above using Pf specific antibodies to CSP (1/100 dilution), exported protein 2 (EXP2) (1/250 dilution) and MSP1 (1/500 dilution), and the rabbit Py-ICP antisera generated in this study. Fluorescent staining and images were achieved as above.

Live microscopy of Py-ICP-RFA—SW mice were infected with Py-ICP-RFA for 3-5 days prior to removal of 100 μl of blood via retro-orbital eye bleed. The blood was washed once with 1xPBS and a drop of blood was mounted on a poly-lysine slide coated with 0.5 μg of mouse anti-Ter119 antibody (eBioscience, San Diego, CA). RBCs were allowed to adhere to the slide for 5 min before visualizing the endogenous GFP signal from Py-ICP-RFA with an Olympus 1 × 70 Delta Vision microscope. Images documenting the dynamic nature of Py-ICP-RFA vesicles were recorded (100 total) and movies were compiled using the Softworx movie tool. DIC images were also obtained in the same manner to ensure that the imaged RBCs were non-motile.

Measuring GFP fluorescence intensity

TMP (250μg/ml) was administered to mice via drinking water for 1 day prior to infection with 200μl of Py-ICP-RFA blood stock. Parasites were allowed to grow for 2 days prior to removal of TMP from drinking water. Parasitemia in SW mice infected with Py-ICP-RFA was determined by Giemsa-stained thin blood smear. Blood was obtained by tail clip at 0-, 2-, 24-, 72-, and 96- hrs following removal of TMP and was diluted to a concentration of 5×10^7 infected RBCs/100μl. One hundred microliters of diluted blood was plated in triplicate on a black 96 well luminometer plate (VWR) and average fluorescence intensity was measured at an excitation of 485nm and an emission bandwidth of 508-530nm on spectraMax M2 plate reader (Molecular Devices).

Sporozoite gliding assay

Salivary gland sporozoites were dissected from mosquitoes infected with Py-ICP-myc, Py, or Pb parasites 14 days after an infectious blood meal, and were column purified as previously described (Mack *et al.*, 1978). Purified sporozoites were allowed to glide on a poly-lysine coated glass slide in a wet chamber at 37°C for 1 h and were then imaged by IFA following the same procedures as described above. Mouse anti-CSP antibody was used to image the sporozoite surface and the gliding trail. Rabbit anti-myc and anti-Py-ICP antisera were also used to visualize the expression of Py-ICP in Py-ICP-myc and WT sporozoites, respectively.

Sporozoite invasion assay

Invasion assays were performed as described in (Kaushansky *et al.*, 2012). Briefly, Py sporozoites were incubated without antibody, or with 0.1mg/ml of either Py-ICP AB pre-immune serum, anti-Py-CSP, or Py-ICP AB for 30min. HepG2 cells expressing CD81 (HepG2-CD81) (Silvie *et al.*, 2006) were cultured in DMEM supplemented with 10% FBS. 3×10^5 cells were plated in each well of a 24-well plate, and infected with 1×10^5 Py sporozoites. 90 min after infection, cells were trypsinized, and then fixed with Perm/Fix buffer (BD Biosciences). Cells were blocked in Perm/Wash buffer (BD Biosciences) supplemented with 2% BSA. Additional staining steps were performed in Perm/Wash buffer alone. Cells were then stained with the F26 monoclonal antibody to circumsporozoite protein conjugated to alexa-fluor 488 at 25°C. Parasitized hepatocytes were identified by flow cytometry using a BD-LSRII flow cytometer (BD Biosciences).

Western blotting

Blood stage parasites and salivary gland sporozoites from Py WT, Py-ICP-myc and Py-ICP-RFA (+/− TMP at 72hr post drug removal) parasites were lysed in Mammalian Protein Extraction Reagent (MPER) (Thermo, Rockford, IL) and the total protein concentration was measured at OD_{280} on a Nanodrop spectrophotometer (Thermo, Rockford, IL). One hundred ng of protein was boiled in SDS-PAGE buffer containing 5% w/v beta-mercaptoethanol for 10 min and was pelleted at 13,000 rpm for 1 min. The soluble fraction was then electrophoresed through an SDS-polyacrylamide (4-20% gradient) gel (Thermo Scientific, Rockford, IL) and was transferred to a PVDF membrane. The membrane was probed with primary antibodies to anti-Py-ICP, c-myc, GFP, and HA antibodies followed by IRDye 680 or 700 secondary antibodies (LI-COR Biotechnology, Lincoln, NE). Protein bands were detected by scanning the membrane on an Odyssey imaging system (LI-COR Biotechnology, Lincoln, NE).

N-terminal sequencing

Recombinant Py-ICP isolated from *E. coli* was electrophoresed through an SDS-polyacrylamide (4-20% gradient) gel (Thermo Scientific, Rockford, IL). The gel was stained

with GelCodeBlue staining reagent (Thermo Scientific, Rockford, IL) to visualize protein bands. Py-ICP's two bands were cut from the gel and N-terminal sequencing was done by automated Edman Degradation on an Applied Biosystems Procise HT (Edman Chemical Sequencing, Harvard University, Boston, MA).

Immunoprecipitation and mass spectrometry

Five experimental and four control co-immunoprecipitations were completed as described in Supplementary Table 1. Lysates of Py, Py-ICP-myc, Py-GFP, and Py-ICP-RFA blood stage parasites were prepared as described above. Py-ICP-myc and Py-GFP (negative control) lysates were run through columns containing anti-myc bound agarose beads from the Pierce c-Myc Tag IP/Co-IP Kit (Thermo Scientific, Rockford, IL). Columns were washed and eluted as per the manufacturer's instructions. RFA-tagged Py-ICP was pulled-down via indirect co-immunoprecipitation using a rabbit anti-GFP antibody (Invitrogen, Carlsbad, CA) and Dynabeads bound with goat anti-rabbit IgG (Invitrogen, Carlsbad, CA). Lysates were first pre-cleared with the Dynabeads for 20 min at 4°C. Pre-cleared lysate was then incubated with a mixture of 20 μl of anti-mouse or rabbit IgG coated Dynabeads and 2 μg of antibody (as described in Figure S2) for 1-3 hr at 4°C. Beads were washed three times with MPER and the bound protein complexes were eluted by boiling the beads in 50 μl of 2x sample buffer for 5 min. SDS-PAGE and western blotting with the Py-ICP antibody was carried out on small portion of the sample (5 μl or $1/10^{th}$ the volume of the total) to confirm the presence of Py-ICP in the lysates (Supplementary Figure S7). The remaining portion of the sample was electrophoresed 1 cm into a SDS-polyacrylamide gel and the excised protein band was analyzed by tandem mass spectrometry (MS/MS) (Fred Hutchinson Cancer Research Center, Seattle, WA). Briefly, the protein samples were digested with trypsin, and the proteolyzed peptides were subjected to MS/MS on a ThermoElectron LTQ electrospray ionization ion trap mass spectrometer (Thermo Scientific, Rockford, IL). The resulting MS/MS data were compared to a protein database of Py and Pb proteins via automated protein database searching from PlasmoDB (www.plasmodb.org). Proteins with multiple unique peptide hits detected in at least two independent immunoprecipitations were reported.

Supplementary Material

Refer to Web version on PubMed Central for supplementary material.

Acknowledgments

This work was supported by R01 AI053709. We would like to thank Dr. Phil Rosenthal for kindly providing the Pf-ICP antibody, Dr. David Narum for the RON4 antibody, and Dr. David Cavanagh for the EXP-2 antibody.

References

Alexander DL, Arastu-Kapur S, Dubremetz JF, Boothroyd JC. Plasmodium falciparum AMA1 binds a rhoptry neck protein homologous to TgRON4, a component of the moving junction in Toxoplasma gondii. Eukaryotic cell. 2006; 5:1169–1173. [PubMed: 16835460]

Aly AS, Matuschewski K. A malarial cysteine protease is necessary for Plasmodium sporozoite egress from oocysts. J Exp Med. 2005; 202:225–230. [PubMed: 16027235]

Azuma H, Paulk N, Ranade A, Dorrell C, Al-Dhalimy M, Ellis E, et al. Robust expansion of human hepatocytes in Fah-/-/Rag2-/-/Il2rg-/- mice. Nat Biotechnol. 2007; 25:903–910. [PubMed: 17664939]

Bergman LW, Kaiser K, Fujioka H, Coppens I, Daly TM, Fox S, et al. Myosin A tail domain interacting protein (MTIP) localizes to the inner membrane complex of Plasmodium sporozoites. J Cell Sci. 2003; 116:39–49. [PubMed: 12456714]

Blackman MJ. Malarial proteases and host cell egress: an ‘emerging’ cascade. Cell Microbiol. 2008; 10:1925–1934. [PubMed: 18503638]

Coppi A, Pinzon-Ortiz C, Hutter C, Sinnis P. The Plasmodium circumsporozoite protein is proteolytically processed during cell invasion. J Exp Med. 2005; 201:27–33. [PubMed: 15630135]

Dasaradhi PV, Mohmmed A, Kumar A, Hossain MJ, Bhatnagar RK, Chauhan VS, Malhotra P. A role of falcipain-2, principal cysteine proteases of Plasmodium falciparum in merozoite egression. Biochem Biophys Res Commun. 2005; 336:1062–1068. [PubMed: 16165088]

Desai PV, Patny A, Gut J, Rosenthal PJ, Tekwani B, Srivastava A, Avery M. Identification of novel parasitic cysteine protease inhibitors by use of virtual screening. 2. The available chemical directory. J Med Chem. 2006; 49:1576–1584. [PubMed: 16509575]

Desai PV, Patny A, Sabnis Y, Tekwani B, Gut J, Rosenthal P, et al. Identification of novel parasitic cysteine protease inhibitors using virtual screening. 1. The ChemBridge database. J Med Chem. 2004; 47:6609–6615. [PubMed: 15588096]

Dhawan S, Dua M, Chishti AH, Hanspal M. Ankyrin peptide blocks falcipain-2-mediated malaria parasite release from red blood cells. J Biol Chem. 2003; 278:30180–30186. [PubMed: 12775709]

Dua M, Raphael P, Sijwali PS, Rosenthal PJ, Hanspal M. Recombinant falcipain-2 cleaves erythrocyte membrane ankyrin and protein 4.1. Mol Biochem Parasitol. 2001; 116:95–99. [PubMed: 11463472]

Eksi S, Czesny B, Greenbaum DC, Bogyo M, Williamson KC. Targeted disruption of Plasmodium falciparum cysteine protease, falcipain 1, reduces oocyst production, not erythrocytic stage growth. Mol Microbiol. 2004; 53:243–250. [PubMed: 15225318]

Farley PJ, Long CA. Plasmodium yoelii yoelii 17XL MSP-1: fine-specificity mapping of a discontinuous, disulfide-dependent epitope recognized by a protective monoclonal antibody using expression PCR (E-PCR). Experimental parasitology. 1995; 80:328–332. [PubMed: 7534725]

Francis SE, Gluzman IY, Oksman A, Banerjee D, Goldberg DE. Characterization of native falcipain, an enzyme involved in Plasmodium falciparum hemoglobin degradation. Mol Biochem Parasitol. 1996; 83:189–200. [PubMed: 9027752]

Hansen G, Heitmann A, Witt T, Li H, Jiang H, Shen X, et al. Structural basis for the regulation of cysteine-protease activity by a new class of protease inhibitors in Plasmodium. Structure. 2011; 19:919–929. [PubMed: 21742259]

Hanspal M, Dua M, Takakuwa Y, Chishti AH, Mizuno A. Plasmodium falciparum cysteine protease falcipain-2 cleaves erythrocyte membrane skeletal proteins at late stages of parasite development. Blood. 2002; 100:1048–1054. [PubMed: 12130521]

Hogg T, Nagarajan K, Herzberg S, Chen L, Shen X, Jiang H, et al. Structural and functional characterization of Falcipain-2, a hemoglobinase from the malarial parasite Plasmodium falciparum. J Biol Chem. 2006; 281:25425–25437. [PubMed: 16777845]

Jongco AM, Ting LM, Thathy V, Mota MM, Kim K. Improved transfection and new selectable markers for the rodent malaria parasite Plasmodium yoelii. Mol Biochem Parasitol. 2006; 146:242–250. [PubMed: 16458371]

Kaushansky A, Rezakhani N, Mann H, Kappe SH. Development of a quantitative flow cytometry-based assay to assess infection by Plasmodium falciparum sporozoites. Molecular and biochemical parasitology. 2012; 183:100–103. [PubMed: 22342965]

Kumar A, Kumar K, Korde R, Puri SK, Malhotra P, Singh Chauhan V. Falcipain-1, a Plasmodium falciparum cysteine protease with vaccine potential. Infect Immun. 2007; 75:2026–2034. [PubMed: 17242063]

Labaied M, Harupa A, Dumpit RF, Coppens I, Mikolajczak SA, Kappe SH. Plasmodium yoelii sporozoites with simultaneous deletion of P52 and P36 are completely attenuated and confer sterile immunity against infection. Infect Immun. 2007; 75:3758–3768. [PubMed: 17517871]

Lee BJ, Singh A, Chiang P, Kemp SJ, Goldman EA, Weinhouse MI, et al. Antimalarial activities of novel synthetic cysteine protease inhibitors. Antimicrob Agents Chemother. 2003; 47:3810–3814. [PubMed: 14638488]

Leiriao P, Albuquerque SS, Corso S, van Gemert GJ, Sauerwein RW, Rodriguez A, et al. HGF/MET signalling protects Plasmodium-infected host cells from apoptosis. Cell Microbiol. 2005; 7:603–609. [PubMed: 15760460]

Lindner SE, Miller JL, Kappe SH. Malaria parasite pre-erythrocytic infection: preparation meets opportunity. Cellular microbiology. 2012; 14:316–324. [PubMed: 22151703]

Mack SR, Vanderberg JP, Nawrot R. Column separation of Plasmodium berghei sporozoites. J Parasitol. 1978; 64:166–168. [PubMed: 342682]

Menard R, Janse C. Gene targeting in malaria parasites. Methods. 1997; 13:148–157. [PubMed: 9405198]

Micale N, Kozikowski AP, Ettari R, Grasso S, Zappala M, Jeong JJ, et al. Novel peptidomimetic cysteine protease inhibitors as potential antimalarial agents. J Med Chem. 2006; 49:3064–3067. [PubMed: 16722625]

Mikolajczak SA, Aly AS, Dumpit RF, Vaughan AM, Kappe SH. An efficient strategy for gene targeting and phenotypic assessment in the Plasmodium yoelii rodent malaria model. Mol Biochem Parasitol. 2008; 158:213–216. [PubMed: 18242728]

Muralidharan V, Oksman A, Iwamoto M, Wandless TJ, Goldberg DE. Asparagine repeat function in a Plasmodium falciparum protein assessed via a regulatable fluorescent affinity tag. Proc Natl Acad Sci U S A. 2011; 108:4411–4416. [PubMed: 21368162]

Na BK, Kim TS, Rosenthal PJ, Lee JK, Kong Y. Evaluation of cysteine proteases of Plasmodium vivax as antimalarial drug targets: sequence analysis and sensitivity to cysteine protease inhibitors. Parasitol Res. 2004; 94:312–317. [PubMed: 15372231]

Pandey KC, Singh N, Arastu-Kapur S, Bogyo M, Rosenthal PJ. Falstatin, a cysteine protease inhibitor of Plasmodium falciparum, facilitates erythrocyte invasion. PLoS Pathog. 2006; 2:e117. [PubMed: 17083274]

Rennenberg A, Lehmann C, Heitmann A, Witt T, Hansen G, Nagarajan K, et al. Exoerythrocytic Plasmodium parasites secrete a cysteine protease inhibitor involved in sporozoite invasion and capable of blocking cell death of host hepatocytes. PLoS Pathog. 2010; 6:e1000825. [PubMed: 20361051]

Rosenthal PJ. Cysteine proteases of malaria parasites. Int J Parasitol. 2004; 34:1489–1499. [PubMed: 15582526]

Salas F, Fichmann J, Lee GK, Scott MD, Rosenthal PJ. Functional expression of falcipain, a Plasmodium falciparum cysteine proteinase, supports its role as a malarial hemoglobinase. Infect Immun. 1995; 63:2120–2125. [PubMed: 7768590]

Schmidt-Christensen A, Sturm A, Horstmann S, Heussler VT. Expression and processing of Plasmodium berghei SERA3 during liver stages. Cell Microbiol. 2008; 10:1723–1734. [PubMed: 18419771]

Shenai BR, Semenov AV, Rosenthal PJ. Stage-specific antimalarial activity of cysteine protease inhibitors. Biol Chem. 2002; 383:843–847. [PubMed: 12108550]

Shenai BR, Sijwali PS, Singh A, Rosenthal PJ. Characterization of native and recombinant falcipain-2, a principal trophozoite cysteine protease and essential hemoglobinase of Plasmodium falciparum. J Biol Chem. 2000; 275:29000–29010. [PubMed: 10887194]

Sijwali PS, Kato K, Seydel KB, Gut J, Lehman J, Klemba M, et al. Plasmodium falciparum cysteine protease falcipain-1 is not essential in erythrocytic stage malaria parasites. Proc Natl Acad Sci U S A. 2004a; 101:8721–8726. [PubMed: 15166288]

Sijwali PS, Rosenthal PJ. Gene disruption confirms a critical role for the cysteine protease falcipain-2 in hemoglobin hydrolysis by Plasmodium falciparum. Proc Natl Acad Sci U S A. 2004b; 101:4384–4389. [PubMed: 15070727]

Sijwali PS, Shenai BR, Gut J, Singh A, Rosenthal PJ. Expression and characterization of the Plasmodium falciparum haemoglobinase falcipain-3. Biochem J. 2001; 360:481–489. [PubMed: 11716777]

Silvie O, Greco C, Franetich JF, Dubart-Kupperschmitt A, Hannoun L, van Gemert GJ, et al. Expression of human CD81 differently affects host cell susceptibility to malaria sporozoites depending on the Plasmodium species. Cellular microbiology. 2006; 8:1134–1146. [PubMed: 16819966]

Singh N, Sijwali PS, Pandey KC, Rosenthal PJ. Plasmodium falciparum: biochemical characterization of the cysteine protease falcipain-2′. Exp Parasitol. 2006; 112:187–192. [PubMed: 16337629]

Sturm A, Amino R, van de Sand C, Regen T, Retzlaff S, Rennenberg A, et al. Manipulation of host hepatocytes by the malaria parasite for delivery into liver sinusoids. Science. 2006; 313:1287–1290. [PubMed: 16888102]

Subramanian S, Hardt M, Choe Y, Niles RK, Johansen EB, Legac J, et al. Hemoglobin cleavage site-specificity of the Plasmodium falciparum cysteine proteases falcipain-2 and falcipain-3. PLoS One. 2009; 4:e5156. [PubMed: 19357776]

Tarun AS, Dumpit RF, Camargo N, Labaied M, Liu P, Takagi A, et al. Protracted sterile protection with Plasmodium yoelii pre-erythrocytic genetically attenuated parasite malaria vaccines is independent of significant liver-stage persistence and is mediated by CD8+ T cells. J Infect Dis. 2007; 196:608–616. [PubMed: 17624848]

Tarun AS, Peng X, Dumpit RF, Ogata Y, Silva-Rivera H, Camargo N, et al. A combined transcriptome and proteome survey of malaria parasite liver stages. Proc Natl Acad Sci U S A. 2008; 105:305–310. [PubMed: 18172196]

Turk B, Stoka V. Protease signalling in cell death: caspases versus cysteine cathepsins. FEBS Lett. 2007; 581:2761–2767. [PubMed: 17544407]

van de Sand C, Horstmann S, Schmidt A, Sturm A, Bolte S, Krueger A, et al. The liver stage of Plasmodium berghei inhibits host cell apoptosis. Molecular microbiology. 2005; 58:731–742. [PubMed: 16238623]

Vaughan AM, Mikolajczak SA, Wilson EM, Grompe M, Kaushansky A, Camargo N, et al. Complete Plasmodium falciparum liver-stage development in liver-chimeric mice. The Journal of clinical investigation. 2012; 122:3618–3628. [PubMed: 22996664]

Vaughan AM, O'Neill MT, Tarun AS, Camargo N, Phuong TM, Aly AS, et al. Type II fatty acid synthesis is essential only for malaria parasite late liver stage development. Cellular microbiology. 2009; 11:506–520. [PubMed: 19068099]

Wickert H, Wissing F, Andrews KT, Stich A, Krohne G, Lanzer M. Evidence for trafficking of PfEMP1 to the surface of P. falciparum-infected erythrocytes via a complex membrane network. Eur J Cell Biol. 2003; 82:271–284. [PubMed: 12868595]

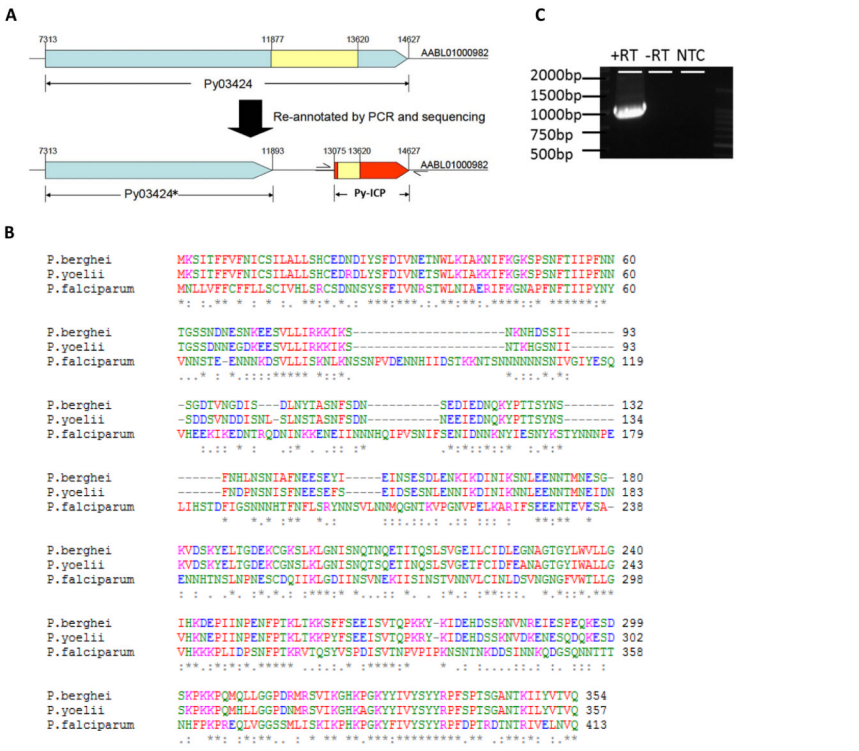

Figure 1. Identification of the Py-ICP gene and alignment of Py-ICP with its orthologs in other *Plasmodium* species

(A) The PY03424 gene from PlasmoDB was re-annotated through RT-PCR and sequencing. The currently annotated PY03424 gene comprises two separate genes: PY03424* and Py-ICP. Introns are shown in yellow and exons are in blue (PY03424*) or red (ICP). (B) The sequence of the re-annotated Py-ICP was aligned with its Pf and Pb orthologs using CLUSTALW. (C) Reverse transcriptase (RT) PCR on Py-ICP mRNA using primers specific for the 5′ and 3′ untranslated regions as designated by arrows in (A). A single band is detected when RT is included in the reaction, but is absent when RT is removed (-RT) and in the non-template control (NTC).

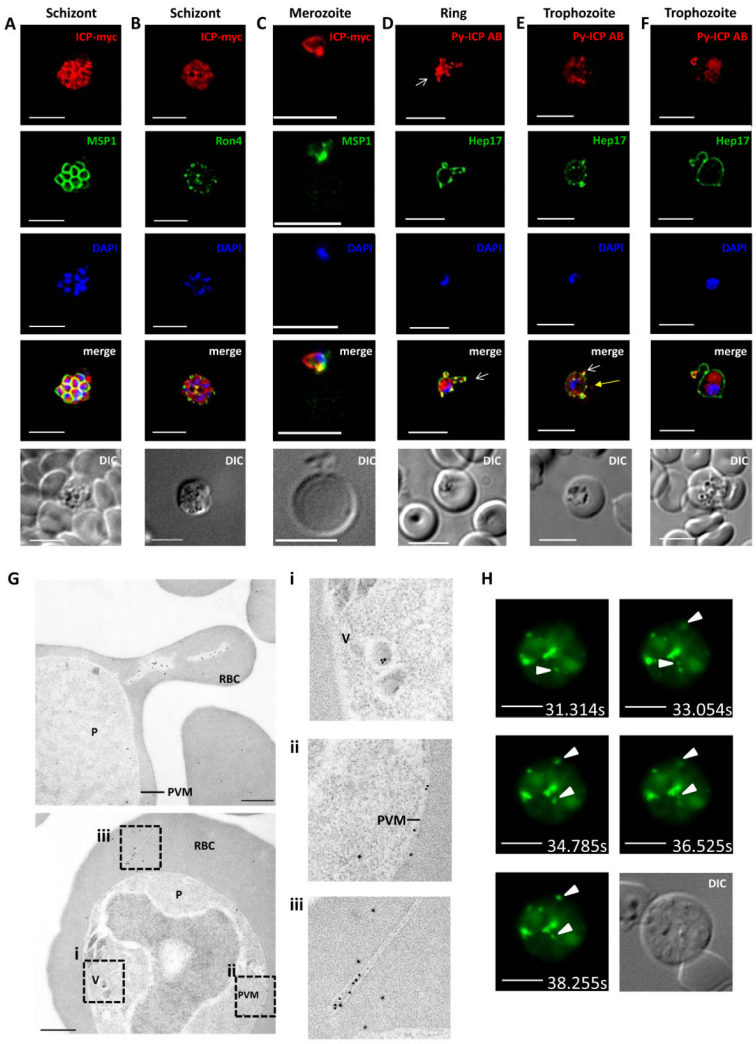

Figure 2. Py-ICP expression and localization in blood stages

The expression of ICP in blood stages was visualized using IFA (A-F), immunoelectron microscopy (IEM) (G), and live fluorescent microscopy (H). (A, B) Py-ICP-myc schizonts were imaged with antibodies to c-myc (red), MSP1 (A, green) or the rhoptry neck marker RON4 (B, green). (C) Py-ICP-myc merozoite invading an erythrocyte. Merozoites were stained with antibodies against c-myc (red) and MSP1 (green). (D thru F) WT blood stage parasites at the ring (D) or trophozoite (E-F) developmental stages were imaged with antibodies to Py-ICP (red) and the PVM marker Hep17 (green). Vesicular structures associated with the PV (Hep17 positive) are indicated by white arrows (D-F), or in Hep17-negative structures with yellow arrow in (E). DNA was imaged with DAPI. Scale bar: 5 μm. (G) IEM of Py-ICP in erythrocytes infected with Py WT parasites. Areas in (F) were magnified 2.5x (dashed box) to show details of ICP localization in parasite-internal vesicles (i), in the PV (ii) and in exomembrane structures within the infected erythrocyte (iii). Scale bar: 500 nm. (H) Live imaging was used to visualize the GFP signal from Py-ICP-RFA in infected erythrocytes. In addition to the GFP signal, DIC images were collected from the same z-stack. Pictures are time stamped and arrows indicate highly mobile ICP-positive punctate structures. Scale bars: 5 μm. Supplemental Movies 1 and 2 show the mobile structures.

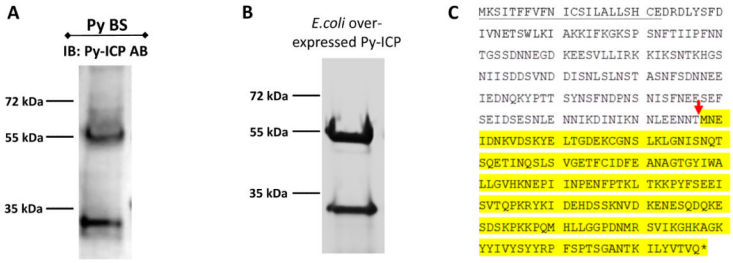

Figure 3. ICP is processed during parasite development

(A) Western blot of Py blood stage lysates with antibody to Py-ICP. Note that two protein bands were detected indicating ICP processing. (B) Recombinant Py-ICP was over-expressed in *E. coli*, column purified, separated by SDS-PAGE and stained with Coomassie (Gelcode blue). Py-ICP is also processed in this bacterial system. (C) The ICP cleavage site, marked by a red arrow, was determined by N-terminal sequencing. The signal peptide sequence is underlined and the processed C-terminal fragment sequence is highlighted in yellow.

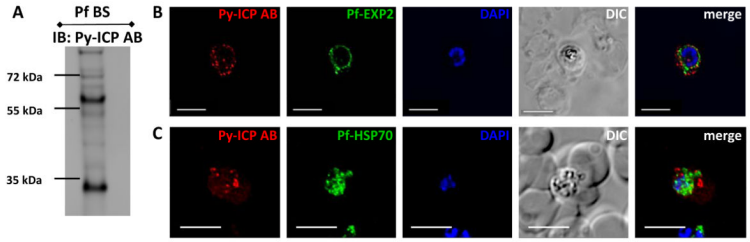

Figure 4. Pf-ICP expression in parasite blood stages

(A) Western blot of lysate from Pf infected blood stages using the Py-ICP antibody. Immunoblotting (IB) reveals that Pf-ICP is processed. (B and C**)** Pf blood stages were imaged by IFA with antibodies to Py-ICP and Pf-EXP2 (B) or HSP70 (C). IFAs depict Pf-ICP localizing to exomembrane structures in the RBC.

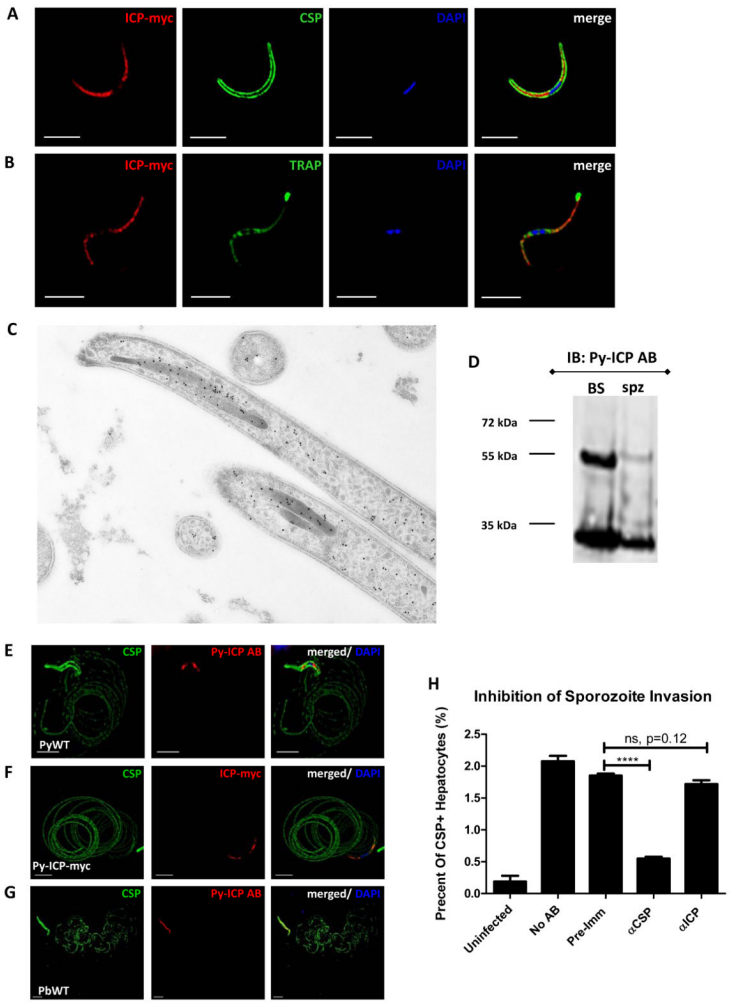

Figure 5. Py-ICP expression and localization in salivary gland sporozoites

(A) Isolated sporozoites were fixed on slides and Py-ICP-myc was localized by IFA with an anti-myc antibody and sporozoites were co-stained with anti-CSP. (B) Micronemal secretion was induced by incubation of Py-ICP-myc sporozoites with RPMI with 20% FCS for 30 min prior to fixation. Sporozoites were then stained with antibodies to myc and the micronemal protein TRAP. (C) Higher resolution localization of Py-ICP-myc in the sporozoite was determined by IEM with an anti-myc antibody (dots). Py-ICP-myc localizes to the rhoptries, but is also found scattered in the sporozoite. (D) Western blot of lysate from Py-ICP-myc sporozoite and blood stage parasites probed with an anti-myc antibody (αmyc). Immunoblots show that Py-ICP is also processed in sporozoites. (E thru G) ICP is not found in trails deposited by gliding sporozoites. For gliding analysis, Py WT (E) and Py-ICP-myc (F) and Pb WT salivary gland sporozoites (G) were isolated by column purification and allowed to glide on poly-lysine treated slides. Trails were detected by IFA using antibodies to CSP (green, E thru G), ICP (red, E and G) and myc (red, F). DNA was imaged with DAPI. Scale bar: 5 μm. (H) Sporozoite invasion assay. *P. yoelii* WT salivary gland sporozoites were incubated without antibody (No AB), or with 0.1mg/ml of the following: Py-ICP AB pre-immune serum (pre-immune), anti Py-CSP (αCSP), or Py-ICP antisera (αICP). After 30 minutes of incubation at room temperature, sporozoites were used to infect HepG2:CD81 cells for 90min at 37°C. Cells were harvested, blocked, and stained with an anti-CSP antibody conjugated to Alexa fluor-488 and analyzed by flow cytometry.

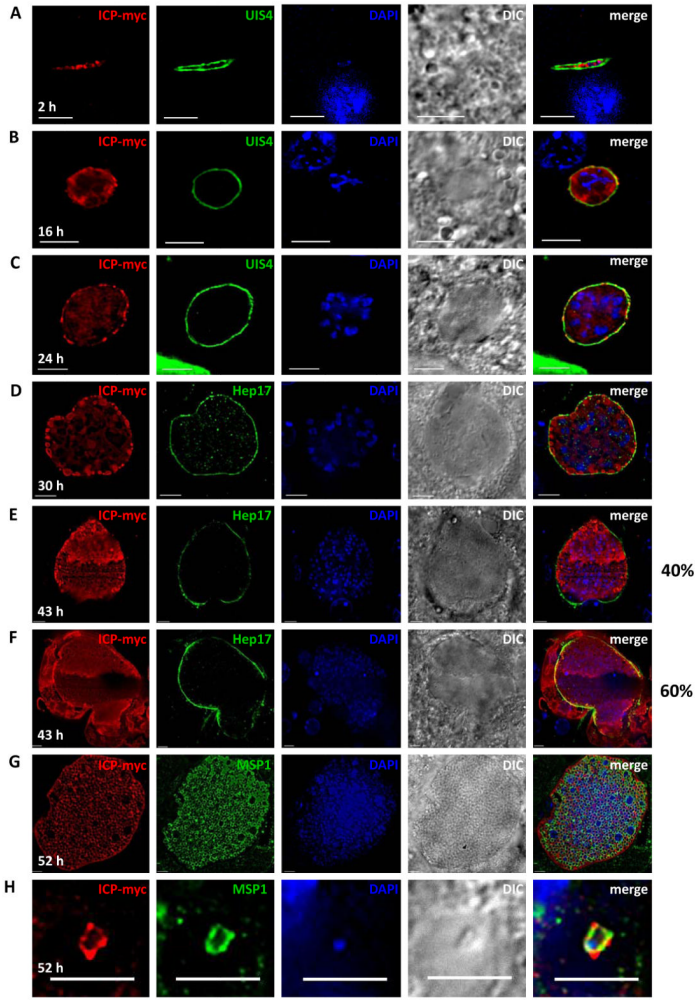

Figure 6. Py-ICP localizes to the parasite cytoplasm and PV during liver stage development and is released into the hepatocyte cytoplasm late in liver stage development

Py sporozoites were intravenously injected into BALB/c mice to study liver stage development in vivo. Liver stages were imaged by IFA at 2- (A), 16- (B), 24- (C), 30- (D), 43- (E and F) and 52- (G and H) hr pi. Antibodies used to detect liver stage parasites included the Py-ICP, the PVM markers UIS4 (A, B and C) and Hep17 (D thru F), the merozoite surface marker MSP1 (G and H). Note that at 43 hr pi, the expression of ICP was detected exclusively inside the parasite PV (40% of liver stages, E) and also in the hepatocyte cytoplasm after PVM breakdown (60% of liver stages, F). Note that at 52 hr pi, ICP was observed on the surface of exoerythrocytic merozoites (G and H). DAPI was used to image DNA and DIC images were also captured. Scale bar: 5 μm.

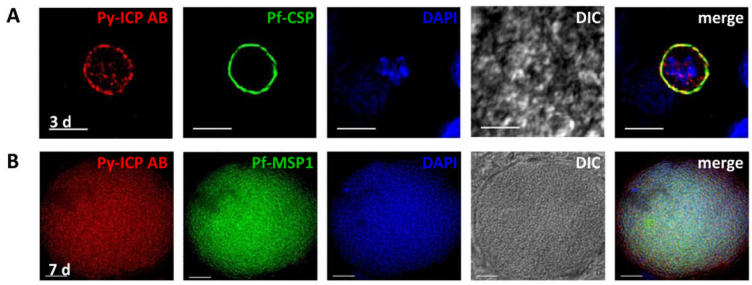

Figure 7. Expression pattern of Pf-ICP in liver stages

(A-B) Pf liver stages from FRG HuHep infected mice were imaged by IFA with Py-ICP antisera (A and B) and antibodies against Pf -CSP (A) and MSP1 (B). DAPI was used to stain host and parasite DNA. DIC and fluorescent images were captured and processed using deconvolution. Scale bar is 5 μm (A) and 10 μm (B).

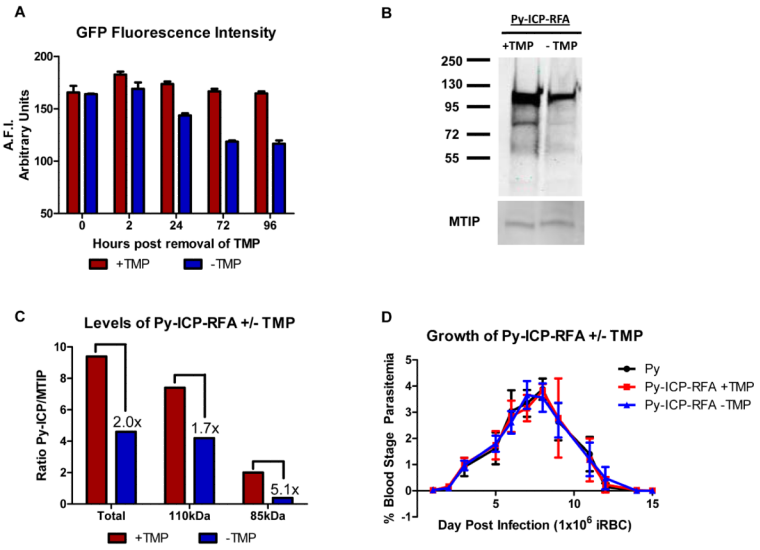

Figure 8. Destabilization reduces Py-ICP levels but does not affect blood stage growth *in vivo*

(A) Monitoring de-stabilization of Py-ICP-RFA by GFP fluorescence intensity. SW mice on TMP were infected with Py-ICP-RFA parasites and parasites were allowed to propagate for 48hrs at which point TMP was removed from a subset of mice (Time 0). Blood was collected from mice +/− TMP at 0-, 2-, 24-, 72-, and 96- hrs following removal of drug and the average fluorescent intensity (A.F.I.) of GFP from 5×10^5 infected RBCs was determined using a fluorescence plate reader. A.F.I. is expressed as arbitrary units. (B) Representative western blot analysis of Py-ICP BS parasite lysates from mice treated with (+TMP) or without TMP (−TMP). ICP expression was detected by anti-HA antibody. The gel was also probed with a rabbit polyclonal antibody against the myosin tail interacting protein (MTIP) (Bergman *et al.*, 2003) for loading control. (C) Bar graph depicting the densitometric ratio of ICP/MTIP from the western blot. Ratios of either total, un-processed (110kDa), or processed (85kDa) protein are depicted. Numbers indicate the fold reduction of protein following removal of TMP. These results are representative of 3 independent experiments. (D) Reduction of ICP levels does not impact blood stage replication. BALB/cJ mice were infected with Py or Py-ICP-RFA parasites in the presence or absence of TMP and blood stage parasitemia was monitored via Geimsa staining of peripheral blood smears. Py-ICP-RFA parasites had a similar growth rate and parasitemia to WT Py regardless of whether the Py-ICP-RFA was being stabilized by TMP.

Table 1

Results of mass spectrometry of proteins pulled down by immunoprecipitation of Py-ICP[a]

Gene ID	Description[b]	Times observed[c] (N=5)	Peptide hits[d]
PY03424	Cysteine protease inhibitor ICP	**5**	**34, 24, 6, 4, 4**
PY00783	Cysteine protease berghepain-2. Ortholog of Falcipain 2^{Pf} and 3^{Pf}.	**5**	**11, 7, 10, 10, 3**
PY03267	Unknown protein, putative. Orthologs are annotated as Golgi organization & biogenesis factor^{Pf} and proteosome regulatory component^{Pb,Pc}.	**2**	**1, 3**
PY01075 [e]	GTPase, Rab18, putative.	**2**	**1, 2**
PY05916	Multiprotein bridging factor type 1, putative.	**2**	**2, 2**
PY01361	Conserved Plasmodium protein, unknown function. Contains WD-40 domains.	**2**	**1, 2**

[a] Proteins were present in at least two immune-precipitations, but not in any of the experimental controls. List does not include ribosomal or heatshock proteins.

[b] Description based on annotations in PlasmoDB. The annotations of orthologous proteins from *P. falciparum* (Pf), *P. berghei* (Pb) and *P. chabaudi* (Pc) are denoted when available.

[c] Determined by the presence of protein in five independent experiments

[d] Total peptide hits observed in each pulldown where protein was observed.

[e] This gene is currently misannotated for *P. yoelii*. Peptide hits correspond to the protein encoded by the syntenic *P. berghei* gene PBANKA_122330